

HarmonyIQA: Pioneering Benchmark and Model for Image Harmonization Quality Assessment

Zitong Xu, Huiyu Duan, Guangji Ma, Liu Yang, Jiarui Wang, Qingbo Wu,
Xionghuo Min, Guangtao Zhai, Patrick Le Callet

Abstract—Image composition involves extracting a foreground object from one image and pasting it into another image through Image Harmonization Algorithms (IHAs), which aim to adjust the appearance of the foreground object to better match the background. Existing image quality assessment (IQA) methods may fail to align with human visual preference on image harmonization due to the insensitivity to minor color or light inconsistency. To address the issue and facilitate the advancement of IHAs, we introduce the first Image Quality Assessment Database for image Harmony evaluation (HarmonyIQAD), which consists of 1,350 harmonized images generated by 9 different IHAs, and the corresponding human visual preference scores. Based on this database, we propose a Harmony Image Quality Assessment (HarmonyIQA), to predict human visual preference for harmonized images. Extensive experiments show that HarmonyIQA achieves state-of-the-art performance on human visual preference evaluation for harmonized images, and also achieves competing results on traditional IQA tasks. Furthermore, cross-dataset evaluation also shows that HarmonyIQA exhibits better generalization ability than self-supervised learning-based IQA methods. Both HarmonyIQAD and HarmonyIQA will be made publicly available upon paper publication.

Index Terms—image quality assessment, image harmonization, large multimodal model

I. INTRODUCTION

Image composition refers to the technique of extracting a foreground object from one image and integrating it into another to create a synthesized composite image [1]. However, this process often introduces inconsistencies in statistical attributes such as color and lighting between the foreground and background. These discrepancies can result in composite images that appear unrealistic and visually disharmonious [2]. Image harmonization algorithms (IHAs) address this issue by adjusting the appearance of the foreground to better match the background, thereby producing more natural and harmonious composite images, as shown in Fig. 1.

IHAs can be broadly categorized into generative image harmonization algorithms (GIHAs) and non-generative image harmonization algorithms (NGIHAs). Some GIHAs [3], [4] leverage Generative Adversarial Networks (GANs) [5], while others [6]–[8] employ diffusion models [9]. More recently, [8] has garnered significant attention for its impressive performance in precise illumination manipulation with diffusion model. However, these GIHAs typically rely on self-supervised learning, where ground truths are unavailable [7], so it is difficult to evaluate GIHAs. In contrast, NGIHAs are typically trained on datasets generated by altering the style of the foreground in real images [1], [2], [10], [11]. These approaches benefit from the availability of real images as ground truth, enabling quality evaluation through similarity

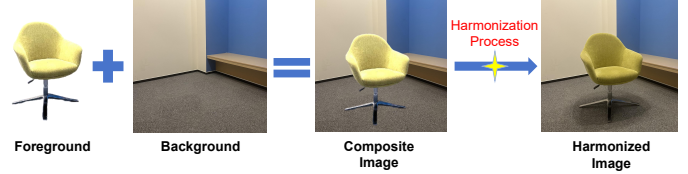


Fig. 1. Example of a composite image and the harmonization process.

metrics. However, such similarity-based evaluation methods struggle to align with human visual preference. Therefore, there is an urgent need for an effective image quality assessment (IQA) method tailored to the harmonization task, which aligned closely with human perception and applicable to the evaluations of NGIHAs and GIHAs.

Existing IQA methods can be broadly classified into two categories: full-reference (FR) IQA and no-reference (NR) IQA. FR IQA relies on reference images for comparison, and many classical methods have been proposed in the literature [13]–[21]. With the rapid advancements in deep neural networks (DNNs), many studies [22]–[24] have utilized learning-based methods and achieved outstanding performance. Nevertheless, in practice, FR IQA is not applicable to evaluate the GIHAs due to the lack of reference images. For NR IQA, traditional methods such as [25]–[29] generally exhibit limited performance. Therefore, learnable NR IQA received more significant attention in recent years, with a variety of works emerging [30]–[38], including convolution neural network (CNN) based IQA models and contrastive language-image pretraining (CLIP) based IQA models. Recently, with the rapid development of large language models (LLMs) and vision-language pre-training techniques, some large multimodal models (LMMs) have proven effective in describing image quality [39]. However, fine-grained IQA, especially in predicting accurate scores of human visual preference, remains a critical challenge for these LMMs.

In this paper, we address the evaluation of IHAs from the perspective of perceptual quality. Firstly, we construct the first Image Quality Assessment Database for image Harmony evaluation (HarmonyIQAD), including 1350 images, which can be divided into two subsets including a NGIHAs subset and a GIHAs subset. Each subset includes harmonized images generated from representative NGIHAs or GIHAs. Then, we recruit a group of experienced researchers in the field of image-processing to subjectively evaluate the harmonization quality of each image in HarmonyIQAD and obtained MOSS.

Based on HarmonyIQAD, we propose the first a Harmony

TABLE I
AN OVERVIEW OF IHAS SELECTED TO CONSTRUCT OUR HARMONYIQAD.

Model	Non-generation IHAs					Generation IHAs			
	L&E [12]	DoveNet [2]	CDT [10]	PCT [1]	DucoNet [11]	ObjectStitch [7]	PHD [4]	PHDiffusion [6]	IC-Light [8]
Year	2007.10	2020.06	2022.09	2023.06	2023.10	2023.05	2023.06	2023.08	2024.06
Method	Color Statistics	CNN	U-Net	Transformer	U-Net	Diffusion	GAN	Diffusion	Diffusion
Resolution	256×256	256×256	2048×2048	256×256	1024×1024	512×512	512×512	512×512	1024×1024

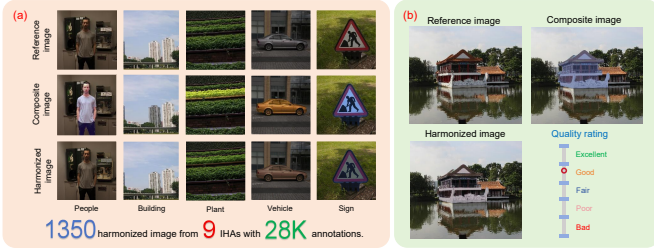


Fig. 2. An overview of the content and rating GUI of HarmonyIQAD. (a) Example images from our database, which contains reference images, composite images and harmonization-processed images. (b) The illustration of GUI for subjective rating.

Image Quality Assessment (HarmonyIQA). HarmonyIQA is built upon a LMM [40] and incorporates instruction tuning [41] and low-rank adaptation (LoRA) [42] techniques. A double-stage training is used to achieve the better score regression. Experimental results demonstrate that HarmonyIQA outperforms all the state-of-the-art FR IQA and NR IQA methods on HarmonyIQAD, and achieves strong performance on other IQA datasets, highlighting its potential as a leading general-purpose IQA method. The key contributions of this work include:

- We construct the HarmonyIQAD, the first image harmonization quality database that contains 1350 harmonized images with over 28K subjective quality ratings.
- We propose HarmonyIQA, the first evaluator capable of fine-grained image harmonization quality scoring, which is also effective for general image quality assessment.
- The extensive experimental results on HarmonyIQAD and other IQA datasets manifest the state-of-art performance of the proposed HarmonyIQA.

II. IMAGE HARMONIZATION QUALITY DATABASE

In this section, we introduce the proposed HarmonyIQAD. This database comprises 150 composite images, 1,350 harmonization-processed images, 150 reference images, and 28,350 human ratings of image quality. The HarmonyIQAD encompasses a broad range of image content, providing a comprehensive resource for evaluating the quality of image harmonization.

A. Image Collection

The ccHarmony dataset [43] forms the basis of our image collection, containing real-world images where foreground objects are placed under varying illumination conditions to create composite images. We selected 150 pairs of composite and reference images, covering diverse foreground objects and color styles. These composite images were processed by 5 NGIHAs, including L&E [12], DoveNet [2], CDT [10], PCT [1] and DucoNet [11], as well as 4 NGIHAs, namely

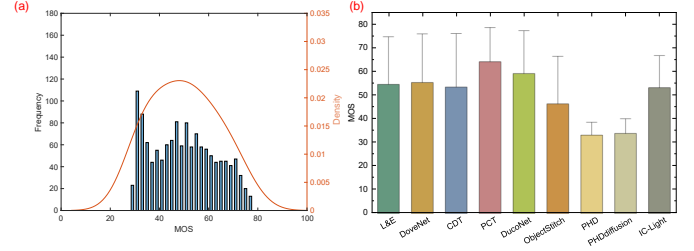


Fig. 3. (a) MOSs distribution in HarmonyIQAD. (b) Mean and standard deviation of the MOSs for each IHAs.

ObjectStitch [7], PHD [4], PHDiffusion [6] and IC-Light [8]. The details of these methods are shown in TABLE I. The harmonized images form the GIHAs and NGIHAs subsets, together with the composite and reference images, creating the HarmonyIQAD, as shown in Fig. 2(a).

B. Subjective Experiment Setup

To evaluate image harmonization quality, we conduct a subjective experiment based on the HarmonyIQAD database. Each time, participants are presented with three images: the harmonized image, composite image, and reference image. They provide a overall quality rating for the harmonized image on a five-point scale, based on three criteria including harmonization effectiveness, content authenticity, and foreground detail preservation. This is because that a good image harmonization algorithm should not only harmonize the composite image, but also maintain the foreground object authenticity and details.

The experiment is conducted using a Python-based GUI displayed on a calibrated LED monitor with a resolution of 3840×2160 , with images shown at their original resolution in random order. A total of 21 professional annotators, seated 2 feet from the monitor in a controlled environment, complete the study in 9 sessions, each under 30 minutes, to minimize fatigue.

C. Subjective Data Analysis

We follow the guidelines outlined in [44] to identify and exclude outliers, as well as to reject subjects who provide unreliable ratings. An individual rating for an image is considered an outlier if it falls outside 2 standard deviations (if normal) or $\sqrt{20}$ standard deviations (if not normal) from the mean rating of that image. A subject is excluded if over 5% of their ratings are outliers. As a result, no subject was excluded based on this criterion and about 2.72% of the total subjective ratings are removed. The remaining valid ratings are converted

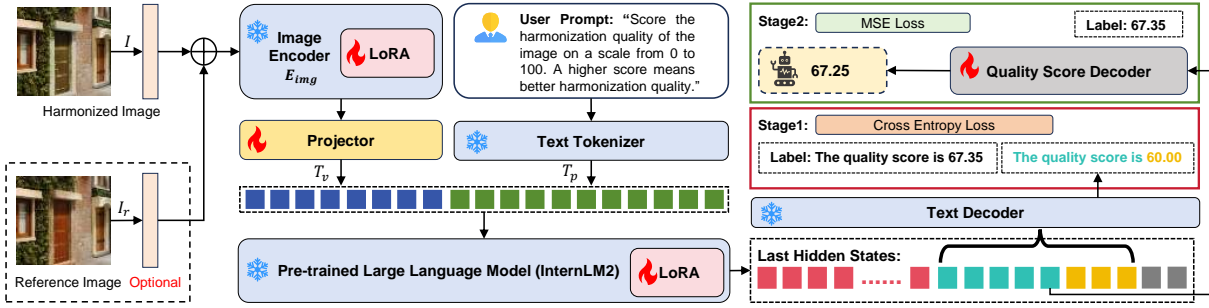


Fig. 4. The HarmonyIQA model consists of two encoders: a visual encoder for extracting image features and a text encoder for processing user prompt features. These features are aligned by a trainable projector and passed into a pre-trained LLM, from which the last hidden states are selected. In the first training stage, these hidden states are decoded through a text decoder, with the text labels and cross-entropy loss used for training. In the second training stage, the hidden state representing the token just before the score is decoded through a quality score decoder, with the score number and mean squared error loss used for training. LoRA weights are introduced to the vision decoder and LLM to adapt the model for the quality assessment task.

into Z-scores, then linearly scaled to the range [0,100]. The final MOS is calculated as followings:

$$z_{ij} = \frac{r_{ij} - \mu_i}{\sigma_i}, z_j = \frac{1}{N_j} \sum_{i=1}^{N_j} z_{ij}, MOS_j = \frac{100(z_j + 3)}{6} \quad (1)$$

where where r_{ij} is the raw rating given by the i -th subject to the j -th image, μ_i is the mean rating and σ_i is the standard deviation provided by the i -th subject and N_j is the number of valid ratings for the j -th image.

Based on the MOSs, we further analyze the collected data. Specifically, we visualize the MOS distributions, as shown in Fig. 3(a). It is clear that the MOS distributions span a wide range. To compare the performance of the Image Harmonization Algorithms (IHAs), we present the mean and standard deviation of the MOSs for the harmonized images produced by each IHAs in Fig. 3(b). The overall performance of all NGIHAs is similar, and generally higher than that of the GIHAs. Among all the IHAs, PCT achieves the best performance, while PHD has the lowest mean score. Moreover, both NGIHAs and GIHAs have large variability, which indicates that the image content significantly affects IHAs effectiveness.

III. IMAGE HARMONIZATION QUALITY EVALUATOR

In this section, we present HarmonyIQA, the first image harmonization quality assessment model, designed to predict harmonization quality scores aligned with human conception.

A. Model Design

Overall Architecture. The overall framework of HarmonyIQA is shown in Fig. 4. It takes both harmonized images and user prompts as input and generates a quality score. HarmonyIQA starts by extracting visual and text features from the images and user prompts, respectively. A weight-frozen vision encoder is used to extract image features, which are then projected into a language space via a projector, generating visual tokens T_v . For text feature extraction, a tokenizer encodes the user prompt into prompt tokens T_p . The concatenated tokens T_v and T_p are fed into a pre-trained LLM. The output consist of last hidden states, which are decoded through a text decoder in the first training stage or a quality score decoder in the second training stage.

Visual Encoding. The image encoder E_{img} is based on the pre-trained vision transformer, InternViT [46]. To align the extracted features with the input space of the LLM, a trainable projector P_{img} with two multi-layer perceptron (MLP) layers is applied. This projects the image features into a language space, generating the visual feature tokens. For an input image I , The process can be formulated as:

$$T_v = P_{img}(E_{img}(I)) \quad (2)$$

where T_v is the visual tokens. HarmonyIQA also supports the input of both harmonized image and reference image I_r to assist the score prediction.

Feature Fusion via the LLM. For a given a user prompt, it is first encoded into text tokens T_p using a text tokenizer. These text tokens T_p are then concatenated with the well-aligned visual tokens T_v to form the input to the LLM. Specifically, the pre-trained InternLM2 [47] is used to combine the visual and text tokens for multimodal learning.

Adaptive Decoding The last hidden states output by the LLM are decoded by text decoder firstly. Once the model is capable of generating responses in the desired format and content, the hidden state representing the token just before the score is then passed to a quality score decoder. This decoder, consisting of two MLPs, is employed in the second training stage to yield a more precise quality score.

B. Fine-tuning Techniques

Instruction Tuning. Many recent works have demonstrated the effectiveness of using instruction-tuning strategies for better performance to finish new task [41]. As shown in Fig. 4, our user prompt includes clear and explicit problem descriptions, maximizing the model’s inference capabilities and enabling HarmonyIQA to accurately respond to specific requirements when performing tasks.

LoRA Adaptation. To enhance the performance of HarmonyIQA, we employ the LoRA technique [42] to pre-trained LMM for efficient model adaptation. LoRA models the changes $\Delta W \in R^{d \times k}$ for each layer’s $W \in R^{d \times k}$ as $\Delta W = AB$, where $A \in R^{d \times r}$ and $B \in R^{k \times r}$. The rank r is constrained much smaller than d and k to achieve parameter efficiency. Given the original output $h = Wx$, the forward pass of LoRA is $h = Wx + \Delta Wx = (W + AB)x$. With

TABLE II

PERFORMANCE OF FR IQA METHODS AND THE PROPOSED HARMONYIQA (FR) ON HARMONYIQAD. THE BEST RESULTS ARE HIGHLIGHTED IN RED, AND THE SECOND-BEST RESULTS ARE HIGHLIGHTED IN BLUE.

Dataset Method/Metrics	All HarmonyIQAD			NGIHAs Subset			GIHAs Subset		
	SRCC	KRCC	PLCC	SRCC	KRCC	PLCC	SRCC	KRCC	PLCC
MSE	0.5696	0.3976	0.4371	0.3171	0.2204	0.3222	0.5018	0.3485	0.3717
PSNR	0.5696	0.3976	0.5688	0.3171	0.2204	0.3503	0.5018	0.3485	0.5658
NQM [15]	0.6095	0.4252	0.6082	0.3319	0.2261	0.3443	0.3999	0.2707	0.4521
MSSIM [16]	0.6566	0.4682	0.6594	0.3100	0.2175	0.3249	0.6165	0.4339	0.6887
SSIM [13]	0.6153	0.4340	0.6160	0.2514	0.1733	0.2843	0.6378	0.4496	0.7201
FSIM [14]	0.6487	0.4605	0.6536	0.2883	0.2006	0.3051	0.6179	0.4337	0.7035
FSIMC [14]	0.6655	0.4746	0.6620	0.3533	0.2445	0.3956	0.6160	0.4324	0.7061
IFC [17]	0.5076	0.3438	0.3603	0.0833	0.0548	0.1184	0.6714	0.4700	0.7541
VIF [18]	0.5059	0.3461	0.5492	0.1597	0.1064	0.1525	0.6638	0.4656	0.7632
GSI [19]	0.6155	0.4337	0.6147	0.2797	0.1934	0.2860	0.6065	0.4265	0.6829
SCSSIM [45]	0.6467	0.4588	0.6499	0.2827	0.1958	0.3301	0.6294	0.4449	0.7092
GMSD [20]	0.6817	0.4910	0.6840	0.2968	0.2060	0.3059	0.5979	0.4242	0.6843
GMSM [20]	0.6066	0.4275	0.6061	0.2601	0.1788	0.2570	0.6232	0.4370	0.6933
VSI [21]	0.6705	0.4812	0.6692	0.4892	0.3401	0.4975	0.5521	0.3876	0.6460
LPiPS (squeeze) [22]	0.5568	0.3903	0.5262	0.4985	0.3499	0.5002	0.5924	0.4151	0.5177
LPiPS (alex) [22]	0.5754	0.4051	0.6012	0.5199	0.3662	0.5503	0.5199	0.3662	0.5144
LPiPS (vgg) [22]	0.5300	0.3707	0.5611	0.3543	0.2427	0.3368	0.6461	0.4553	0.7154
ST-LPiPS (alex) [23]	0.4135	0.2839	0.2825	0.3637	0.2472	0.3872	0.3467	0.2382	0.3807
ST-LPiPS (vgg) [23]	0.5104	0.3606	0.5301	0.3570	0.2442	0.4027	0.4443	0.3094	0.5082
AHIQ [24]	0.7670	0.5677	0.7728	0.4213	0.2851	0.4450	0.7114	0.5175	0.7341
HarmonyIQA (FR)	0.7988	0.6128	0.7910	0.5965	0.4217	0.5810	0.7146	0.5414	0.7587

TABLE III

PERFORMANCE OF NR IQA METHODS AND THE PROPOSED HARMONYIQA (NR) ON HARMONYIQAD. THE BEST RESULTS ARE HIGHLIGHTED IN RED, AND THE SECOND-BEST RESULTS ARE HIGHLIGHTED IN BLUE.

Dataset Method/Metrics	All HarmonyIQAD			NGIHAs Subset			GIHAs Subset		
	SRCC	KRCC	PLCC	SRCC	KRCC	PLCC	SRCC	KRCC	PLCC
BIQI [27]	0.0835	0.0574	0.1714	0.0385	0.0273	0.1456	0.2027	0.1372	0.2554
DIIVINE [28]	0.0946	0.0620	0.1492	0.1495	0.0991	0.1552	0.0483	0.0305	0.1322
BRISQUE [26]	0.1238	0.0812	0.2287	0.0809	0.0543	0.2166	0.2661	0.1852	0.2259
BLIINDS-II [29]	0.2339	0.1531	0.3079	0.1069	0.0736	0.1702	0.0371	0.0241	0.0788
NIQE [25]	0.2527	0.1718	0.3111	0.0959	0.0630	0.2267	0.0649	0.0415	0.2027
CNNIQA [30]	0.6215	0.4836	0.6454	0.2286	0.2185	0.3000	0.3952	0.3282	0.4433
WaDIQaM [31]	0.6204	0.4392	0.6308	0.2695	0.1790	0.2892	0.4227	0.2956	0.4473
NIMA [32]	0.5191	0.3911	0.5055	0.2077	0.1778	0.2721	0.3237	0.2537	0.3962
DBCNN [33]	0.6329	0.4432	0.6664	0.1203	0.0787	0.2011	0.5316	0.3671	0.5827
HyperIQA [34]	0.6786	0.4866	0.7041	0.2276	0.1511	0.2410	0.5106	0.3656	0.5265
MANIQA [35]	0.7596	0.5571	0.7583	0.4977	0.3410	0.5265	0.6201	0.4354	0.6630
CLIPiQA [36]	0.6797	0.4822	0.6519	0.2963	0.1935	0.1564	0.3824	0.2571	0.3843
TOPIQ [37]	0.7017	0.5175	0.7047	0.2739	0.1959	0.2767	0.7191	0.5250	0.7583
ARNIQA [38]	0.7046	0.5099	0.7215	0.3036	0.2037	0.3242	0.5797	0.4180	0.6425
HarmonyIQA (NR)	0.7848	0.5888	0.7650	0.7371	0.5465	0.7261	0.8411	0.6533	0.8318

the LoRA, HarmonyIQA can effectively adapt to the image quality scores prediction task.

Double-stage Training We trained HarmonyIQA in two stages. In the first stage, we used cross-entropy loss, with the label being a sentence that includes the quality score. The goal of this stage is to train the model to generate text in the desired format, along with a roughly accurate quality score. However, relying solely on text training does not yield an accurate score result. Therefore, in the second stage, we use Mean Squared Error (MSE) loss, with the label being the quality score number. The objective of this stage is to refine the ability of HarmonyIQA to produce a more accurate quality score.

IV. EXPERIMENTAL EVALUATION

A. Evaluation on HarmonyIQAD

We first split the HarmonyIQAD dataset into training and test sets with a 4:1 ratio. The harmonization-processed images generated by each IHA are allocated according to this same ratio. Then, 20 FR IQA methods and 14 NR IQA methods are selected as baselines for our HarmonyIQA, totally divided into four groups: traditional FR IQA, leaning-based FR IQA, traditional NR IQA and learning-based NR IQA. Performance is

evaluated using three metrics: Spearman rank-order correlation coefficient (SRCC), Kendall rank-order correlation coefficient (KRCC), and Pearson linear correlation coefficient (PLCC). In addition to evaluating on the entire dataset, we also conduct separate evaluations on GIHAs subset and NGIHAs subset.

The results is shown in TABLE. II and TABLE. III. We find that HarmonyIQA outperforms all other IQA methods across all metrics on both the whole and subsets of HarmonyIQAD.

B. Ablation Study

We conduct ablation studies on HarmonyIQAD and its two subsets to evaluate the effectiveness of the core components of HarmonyIQA. The results are presented in TABLE IV.

Effectiveness of LoRA Adaptation. We first demonstrate the effectiveness of LoRA adaptation, as shown in rows 1 to 3 of TABLE IV. The results indicate that applying LoRA to both the vision model and the LLM yields the best performance for the our HarmonyIQA.

Effectiveness of Training Projector Weights. The projector in HarmonyIQA is responsible for projecting vision features into the language space. As shown in row 4 of TABLE IV, training the projector weights results in improved performance.

TABLE IV
ABLATION STUDY OF OUR HARMONYIQAD ON HARMONYIQA AND ITS NGIHAS SUBSET AND GIHAS SUBSET.

Strategy				All HarmonyIQAD		NGIHAs Subset		GIHAs Subset	
LoRA(vision)	LoRA(llm)	Projector Training	Quality Score Decoder	SRCC	PLCC	SRCC	PLCC	SRCC	PLCC
✓				0.6972	0.6795	0.4209	0.4141	0.5487	0.5348
	✓			0.7275	0.7107	0.4240	0.4033	0.5231	0.5844
✓	✓			0.7437	0.7215	0.4328	0.4270	0.5664	0.5925
✓	✓	✓		0.7568	0.7393	0.4374	0.4254	0.6514	0.6771
✓	✓	✓	✓	0.7848	0.7650	0.7371	0.7261	0.8411	0.8318

TABLE V
PERFORMANCE COMPARISON OF STATE-OF-THE-ART NR IQA METHODS AND HARMONYIQA(NR) ON CSIQ [48], TID2013 [49] AND KADID [50] DATABASES. THE BEST RESULTS ARE HIGHLIGHTED IN RED, AND THE SECOND-BEST RESULTS ARE HIGHLIGHTED IN BLUE.

Dataset	CSIQ		TID2013		KADID	
	SRCC	PLCC	SRCC	PLCC	SRCC	PLCC
BRISQUE [26]	0.812	0.748	0.643	0.571	0.528	0.567
NIQE [25]	0.627	0.721	0.315	0.393	0.374	0.428
WaDIQaM [31]	0.852	0.844	0.835	0.855	0.739	0.752
DBCNN [33]	0.946	0.959	0.816	0.851	0.856	0.856
HyperIQA [34]	0.923	0.942	0.840	0.858	0.852	0.845
ARNIQA [38]	0.962	0.973	0.880	0.901	0.908	0.912
HarmonyIQA	0.968	0.977	0.901	0.913	0.935	0.938

TABLE VI
THE CROSS-DATASET EVALUATION RESULTS FOR THE SRCC METRIC USING LIVE [51], CSIQ [48] AND TID2013 [49]. THE BEST SCORES ARE HIGHLIGHTED IN RED.

Train on	Test on	Method		
		HyperIQA [34]	ARNIQA [38]	HarmonyIQA
LIVE	CSIQ	0.744	0.904	0.838
LIVE	TID2013	0.541	0.697	0.784
CSIQ	LIVE	0.926	0.921	0.938
CSIQ	TID2013	0.541	0.721	0.787
TID2013	LIVE	0.876	0.869	0.883
TID2013	CSIQ	0.709	0.866	0.804
Average Performance		0.723	0.830	0.839

Effectiveness of Quality Score Decoder. HarmonyIQA undergoes two stages of training. In the second training stage, a quality score decoder is employed for more accurate quality score regression. Row 5 of TABLE IV demonstrates that adding the quality score decoder significantly improves performance.

C. Evaluation on Existing IQA datasets

We further evaluate the performance of the proposed HarmonyIQA on three additional IQA benchmark datasets: CSIQ [48], TID2013 [49] and KADID [50]. For these three datasets, we follow the same principles of splitting the data into training and test sets with a 4:1 ratio. TABLE V presents that HarmonyIQA achieves state-of-the-art performance across these datasets.

D. Cross-dataset Evaluation

We also conduct cross-database evaluations on three IQA datasets including LIVE [51], CSIQ [48] and TID2013 [49]. The results shown in TABLE VI demonstrate that, compared to two other state-of-the-art IQA methods [34], [38], HarmonyIQA demonstrates superior performance. In particular, while ARNIQA employs self-supervised learning and linear regression, HarmonyIQA exhibits better overall generalization ability over this method.

V. CONCLUSION

In this paper, we present HarmonyIQAD, the first comprehensive image harmonization quality database, which contains

1,350 harmonized images with subjective quality scores. Based on the dataset, we propose HarmonyIQA, which leverages advanced visual encoding techniques, instruction tuning and LoRA tuning, to perform image quality predicting. Extensive experiments on HarmonyIQAD and other widely used IQA datasets demonstrate the excellent performance of HarmonyIQA, highlighting its potential for general image quality assessment application.

REFERENCES

- [1] Julian Jorge Andrade Guerreiro, Mitsuru Nakazawa, and Björn Stenger, "Pct-net: Full resolution image harmonization using pixel-wise color transformations," in *Proceedings of the IEEE Conference on Computer Vision and Pattern Recognition (CVPR)*, 2023, pp. 5917–5926.
- [2] Wenyan Cong, Jianfu Zhang, Li Niu, Liu Liu, Zhixin Ling, Weiyuan Li, et al., "Dovenet: Deep image harmonization via domain verification," in *Proceedings of the IEEE Conference on Computer Vision and Pattern Recognition (CVPR)*, 2020, pp. 8391–8400.
- [3] Zhongyun Bao, Chengjiang Long, Gang Fu, Daquan Liu, Yuanzhen Li, Jiaming Wu, et al., "Deep image-based illumination harmonization," in *Proceedings of the IEEE Conference on Computer Vision and Pattern Recognition (CVPR)*, June 2022, pp. 18542–18551.
- [4] Junyan Cao, Yan Hong, and Li Niu, "Painterly image harmonization in dual domains," in *Proceedings of the Conference on Association for the Advancement of Artificial Intelligence (AAAI)*, 2023, vol. 37, pp. 268–276.
- [5] Ian Goodfellow, Jean Pouget-Abadie, Mehdi Mirza, Bing Xu, David Warde-Farley, Sherjil Ozair, Aaron Courville, and Yoshua Bengio, "Generative adversarial networks," *Communications of the ACM (CACM)*, vol. 63, no. 11, pp. 139–144, Oct. 2020.
- [6] Lingxiao Lu, Jiangtong Li, Junyan Cao, Li Niu, and Liqing Zhang, "Painterly image harmonization using diffusion model," in *Proceedings of the ACM International Conference on Multimedia (ACM MM)*, 2023, pp. 233–241.
- [7] Yizhi Song, Zhifei Zhang, Zhe Lin, Scott Cohen, Brian Price, Jianming Zhang, et al., "Objectstitch: Object compositing with diffusion model," in *Proceedings of the IEEE Conference on Computer Vision and Pattern Recognition (CVPR)*, 2023, pp. 18310–18319.
- [8] Anonymous, "Scaling in-the-wild training for diffusion-based illumination harmonization and editing by imposing consistent light transport," in *Submitted to International Conference on Learning Representations (ICLR)*, 2024, under review.
- [9] Jonathan Ho, Ajay Jain, and Pieter Abbeel, "Denoising diffusion probabilistic models," in *Proceedings of the Advances in Neural Information Processing Systems (NeurIPS)*, H. Larochelle, M. Ranzato, R. Hadsell, M.F. Balcan, and H. Lin, Eds., 2020, vol. 33, pp. 6840–6851.
- [10] Wenyan Cong, Xinhao Tao, Li Niu, Jing Liang, Xuesong Gao, Qihao Sun, et al., "High-resolution image harmonization via collaborative dual transformations," in *Proceedings of the IEEE Conference on Computer Vision and Pattern Recognition (CVPR)*, 2022, pp. 18449–18458.
- [11] Linfeng Tan, Jiangtong Li, Li Niu, and Liqing Zhang, "Deep image harmonization in dual color spaces," in *Proceedings of the ACM International Conference on Multimedia (ACM MM)*, 2023, pp. 2159–2167.
- [12] Jean-Francois Lalonde and Alexei A. Efros, "Using color compatibility for assessing image realism," in *Proceedings of the IEEE International Conference on Computer Vision (ICCV)*, 2007, pp. 1–8.
- [13] Z. Wang, A. C. Bovik, H. R. Sheikh, and E. P. Simoncelli, "Image quality assessment: from error visibility to structural similarity," *IEEE Transactions on Image Processing (TIP)*, vol. 13, no. 4, pp. 600–612, 2004.

- [14] L. Zhang, L. Zhang, X. Mou, and D. Zhang, "Fsim: A feature similarity index for image quality assessment," *IEEE Transactions on Image Processing (TIP)*, vol. 20, no. 8, pp. 2378–2386, 2011.
- [15] N. Damera-Venkata, T. D. Kite, W. S. Geisler, B. L. Evans, and A. C. Bovik, "Image quality assessment based on a degradation model," *IEEE Transactions on Image Processing (TIP)*, vol. 9, no. 4, pp. 636–650, 2000.
- [16] Z. Wang, E. P. Simoncelli, and A. C. Bovik, "Multiscale structural similarity for image quality assessment," in *Proceedings of the Asilomar Conference on Signals, Systems & Computers (ACSSC)*, 2003, vol. 2, pp. 1398–1402.
- [17] H. R. Sheikh, A. C. Bovik, and G. De Veciana, "An information fidelity criterion for image quality assessment using natural scene statistics," *IEEE Transactions on Image Processing (TIP)*, vol. 14, no. 12, pp. 2117–2128, 2005.
- [18] H. R. Sheikh and A. C. Bovik, "Image information and visual quality," *IEEE Transactions on Image Processing (TIP)*, vol. 15, no. 2, pp. 430–444, 2006.
- [19] A. Liu, W. Lin, and M. Narwaria, "Image quality assessment based on gradient similarity," *IEEE Transactions on Image Processing (TIP)*, vol. 21, no. 4, pp. 1500–1512, 2011.
- [20] W. Xue, L. Zhang, X. Mou, and A. C. Bovik, "Gradient magnitude similarity deviation: A highly efficient perceptual image quality index," *IEEE Transactions on Image Processing (TIP)*, vol. 23, no. 2, pp. 684–695, 2013.
- [21] L. Zhang, Y. Shen, and H. Li, "Vsi: A visual saliency-induced index for perceptual image quality assessment," *IEEE Transactions on Image Processing (TIP)*, vol. 23, no. 10, pp. 4270–4281, 2014.
- [22] R. Zhang, P. Isola, A. A. Efros, E. Shechtman, and O. Wang, "The unreasonable effectiveness of deep features as a perceptual metric," in *Proceedings of the IEEE Conference on Computer Vision and Pattern Recognition (CVPR)*, 2018, pp. 586–595.
- [23] Abhijay Ghildyal and Feng Liu, "Shift-tolerant perceptual similarity metric," in *Proceedings of the European Conference on Computer Vision (ECCV)*, 2022, p. 91–107.
- [24] Shanshan Lao, Yuan Gong, Shuwei Shi, Sidi Yang, Tianhe Wu, Jiahao Wang, et al., "Attentions help cnns see better: Attention-based hybrid image quality assessment network," in *Proceedings of the IEEE Conference on Computer Vision and Pattern Recognition (CVPR) Workshops*, June 2022, pp. 1140–1149.
- [25] Anish Mittal, Rajiv Soundararajan, and Alan C. Bovik, "Making a 'completely blind' image quality analyzer," *IEEE Signal Processing Letters (SPL)*, vol. 20, no. 3, pp. 209–212, 2013.
- [26] Anish Mittal, Anush K. Moorthy, and Alan C. Bovik, "Blind/referenceless image spatial quality evaluator," in *Proceedings of the Asilomar Conference on Signals, Systems and Computers (ACSSC)*, 2011, pp. 723–727.
- [27] A. K. Moorthy and A. C. Bovik, "A modular framework for constructing blind universal quality indices," *IEEE Signal Processing Letters (SPL)*, 2009.
- [28] Anush Krishna Moorthy and Alan Conrad Bovik, "Blind image quality assessment: From natural scene statistics to perceptual quality," *IEEE Transactions on Image Processing (TIP)*, vol. 20, no. 12, pp. 3350–3364, 2011.
- [29] Michele A. Saad, Alan C. Bovik, and Christophe Charrier, "Blind image quality assessment: A natural scene statistics approach in the dct domain," *IEEE Transactions on Image Processing (TIP)*, vol. 21, no. 8, pp. 3339–3352, 2012.
- [30] Le Kang, Peng Ye, Yi Li, and David Doermann, "Convolutional neural networks for no-reference image quality assessment," in *Proceedings of the IEEE Conference on Computer Vision and Pattern Recognition (CVPR)*, 2014, pp. 1733–1740.
- [31] S. Bosse, D. Maniry, K.-R. Muller, T. Wiegand, and W. Samek, "Deep neural networks for no-reference and full-reference image quality assessment," *IEEE Transactions on Image Processing (TIP)*, vol. 27, no. 1, pp. 206–219, 2017.
- [32] H. Talebi and P. Milanfar, "Nima: Neural image assessment," *IEEE Transactions on Image Processing (TIP)*, vol. 27, no. 8, pp. 3998–4011, 2018.
- [33] W. Zhang, K. Ma, J. Yan, D. Deng, and Z. Wang, "Blind image quality assessment using a deep bilinear convolutional neural network," *IEEE Transactions on Circuits and Systems for Video Technology (TCSVT)*, vol. 30, no. 1, pp. 36–47, 2020.
- [34] S. Su, Q. Yan, Y. Zhu, C. Zhang, X. Ge, J. Sun, et al., "Blindly assess image quality in the wild guided by a self-adaptive hyper network," in *Proceedings of the IEEE Conference on Computer Vision and Pattern Recognition (CVPR)*, June 2020.
- [35] Sidi Yang, Tianhe Wu, Shuwei Shi, Shanshan Lao, Yuan Gong, Mingdeng Cao, et al., "Maniqa: Multi-dimension attention network for no-reference image quality assessment," in *Proceedings of the IEEE Conference on Computer Vision and Pattern Recognition (CVPR)*, 2022, pp. 1191–1200.
- [36] Jianyi Wang, Kelvin C.K. Chan, and Chen Change Loy, "Exploring clip for assessing the look and feel of images," in *Proceedings of the Conference on Association for the Advancement of Artificial Intelligence (AAAI)*, 2023.
- [37] Chaofeng Chen, Jiadi Mo, Jingwen Hou, Haoning Wu, Liang Liao, Wenxiu Sun, Qiong Yan, and Weisi Lin, "Topiq: A top-down approach from semantics to distortions for image quality assessment," *IEEE Transactions on Image Processing (TIP)*, vol. 33, pp. 2404–2418, 2024.
- [38] Lorenzo Agnolucci, Leonardo Galteri, Marco Bertini, and Alberto Del Bimbo, "Arniqa: Learning distortion manifold for image quality assessment," in *Proceedings of IEEE Winter Conference on Applications of Computer Vision (WACV)*, 2024, pp. 188–197.
- [39] Puyi Wang, Wei Sun, Zicheng Zhang, Jun Jia, Yanwei Jiang, Zhichao Zhang, et al., "Large multi-modality model assisted ai-generated image quality assessment," in *Proceedings of the ACM International Conference on Multimedia (ACM MM)*, 2024, p. 7803–7812.
- [40] Qinghao Ye, Haiyang Xu, Jiabo Ye, Ming Yan, Anwen Hu, Haowei Liu, et al., "mplug-owl2: Revolutionizing multi-modal large language model with modality collaboration," in *Proceedings of the IEEE Conference on Computer Vision and Pattern Recognition (CVPR)*, 2024, pp. 13040–13051.
- [41] Haotian Liu, Chunyuan Li, Qingyang Wu, and Yong Jae Lee, "Visual instruction tuning," in *Proceedings of the Advances in Neural Information Processing Systems (NeurIPS)*, 2023, vol. 36, pp. 34892–34916.
- [42] Edward J. Hu, Yelong Shen, Phillip Wallis, Zeyuan Allen-Zhu, Yuanzhi Li, Shean Wang, et al., "Lora: Low-rank adaptation of large language models," in *Proceedings of the International Conference on Learning Representations (ICLR)*, 2022.
- [43] Li Niu, Linfeng Tan, Xinhao Tao, Junyan Cao, Fengjun Guo, Teng Long, et al., "Deep image harmonization with globally guided feature transformation and relation distillation," in *IEEE International Conference on Computer Vision (ICCV)*, 2023, pp. 7689–7698.
- [44] International Telecommunication Union (ITU), "Methodology for the subjective assessment of the quality of television pictures," Tech. Rep. Rec. ITU-R BT.500-13, International Telecommunication Union (ITU), Jan. 2012.
- [45] K. Gu, G. Zhai, X. Yang, and W. Zhang, "An improved full-reference image quality metric based on structure compensation," in *Proceedings of the conference on Asia-Pacific Signal and Information Processing Association (APSIPA)*, 2012, pp. 1–6.
- [46] Zhe Chen, Jiannan Wu, Wenhai Wang, Weijie Su, Guo Chen, Sen Xing, et al., "Internvl: Scaling up vision foundation models and aligning for generic visual-linguistic tasks," in *Proceedings of the IEEE Conference on Computer Vision and Pattern Recognition (CVPR)*, 2024, pp. 24185–24198.
- [47] InternLM Team, "Internlm: A multilingual language model with progressively enhanced capabilities," 2023, arXiv:2307.09742.
- [48] Eric Cooper Larson and Damon Michael Chandler, "Most apparent distortion: Full-reference image quality assessment and the role of strategy," *Journal of Electronic Imaging (JEI)*, vol. 19, no. 1, pp. 011006, 2010.
- [49] Nikolay Ponomarenko, Lina Jin, Oleg Ieremeiev, Vladimir Lukin, Karen Egiazarian, Jaakko Astola, et al., "Image database tid2013: Peculiarities, results and perspectives," *Signal Processing: Image Communication*, vol. 30, pp. 57–77, 2015.
- [50] Hanhe Lin, Vlad Hosu, and Dietmar Saupe, "Kadid-10k: A large-scale artificially distorted iqa database," in *Proceedings of the International Conference on Quality of Multimedia Experience (QoMEX)*, 2019, pp. 1–3.
- [51] Hamid R. Sheikh, Muhammad F. Sabir, and Alan C. Bovik, "A statistical evaluation of recent full reference image quality assessment algorithms," *IEEE Transactions on Image Processing (TIP)*, vol. 15, no. 11, pp. 3440–3451, 2006.